Simultaneous Optical Links with the Inter-Satellite Omnidirectional Optical Communicator

Alexa Aguilar
Jet Propulsion Laboratory, California Institute of Technology
4800 Oak Grove Dr.
Pasadena, CA 91109
Alexa.C.Aguilar@jpl.nasa.gov

Jose Velazco
Jet Propulsion Laboratory, California Institute of Technology
4800 Oak Grove Dr.
Pasadena, CA 91109
Jose.E.Velazco@jpl.nasa.gov

Kerri Cahoy
Massachusetts Institute of Technology
77 Massachusetts Avenue
Cambridge, MA 02139
kcahoy@mit.edu

Abstract—**As the onboard data volume for smaller platforms such as CubeSats increases, Radio Frequency (RF) communications systems may be unable to adequately support the required downlink demand. Optical communications (lasercom) systems can relieve the data bottleneck as they can support higher data throughput than RF for comparable Size, Weight, and Power (SWaP). Lasercom crosslinks are of particular interest for spacecraft swarms and constellations because they enable additional mission robustness for distributed science observations and remote sensing applications. The Inter-Satellite Omnidirectional optical Communicator (ISOC) is capable of supporting simultaneous lasercom crosslinks between multiple spacecraft at separations of up to thousands of kilometers in orbit. The ISOC architecture features a truncated dodecahedron chassis containing an array of photodetectors and gimbal-less MEMS mirrors, enabling full-duplex communications. The main objectives of the ISOC terminal include: 1) full sky coverage, 2) Gbps data rates, and 3) the ability to maintain multiple simultaneous links. We show ISOC can support up to 12 simultaneous links with the current architecture at 1-Gbps at 200-km separation with 10^{-9} BER. Compared to current lasercom transceivers (i.e., point-to-point), ISOC offers increased throughput performance for similar SWaP. A detailed link budget for both scenarios is presented, and the limiting factors for maximum number of simultaneous links are discussed.**

TABLE OF CONTENTS

1. INTRODUCTION 1
2. ISOC OVERVIEW 2
3. LINK BUDGET 2
4. MULTIPLE ACCESS 3
5. CONCLUSION 6
ACKNOWLEDGEMENTS 6
REFERENCES 6
BIOGRAPHY 8

1. INTRODUCTION

Large systems comprised of highly capable small satellites and CubeSats are becoming increasingly popular with applications to science [1] and communications [2]–[5]. These constellations and swarms are rapidly approaching network-like architectures with thousands of connected spacecraft (nodes). As these systems become increasingly complex and on-orbit data volume increases, higher data rates and levels of autonomy are required to 1.) enable self-directed rapid response and coordination with minimal human-in-the-loop feedback, 2.) perform data routing between nodes for lower latency operations and data offloading, and 3.) increase downlink speeds.

Radio Frequency (RF) communication is bandwidth limited and may not support the data rate demand for network-like systems. Free-Space Optical Communication (FSOC), or lasercom, overcomes bandwidth limitations and offers higher data rates for similar or lower Size Weight and Power (SWaP). Lasercom downlinks can alleviate the throughput bottleneck experienced by RF communications by using the higher available capacity and increasing total data volume sent to Earth during a ground station pass. Optical Inter-Satellite Links (OISLs), or crosslinks, enable data routing to neighboring satellites, which may reduce the total data throughput required during downlink and supports low latency operations. Despite capacity and SWaP advantages, lasercom to date supports single, point-to-point links (i.e., single user operation) which ultimately limits network performance. Despite bandwidth limitations, RF communications is a competitive technology for space-based network architectures due to the ability to support multiple simultaneous links (multiuser operation) through frequency reuse and multiple access protocols. To meet the capacity requirements of space-based networks and leverage advantages of lasercom and RF, multiple access protocols enabling multiuser lasercom are required.

The Jet Propulsion Laboratory is developing a novel lasercom terminal known as the Inter-Satellite Omnidirectional Optical Communicator (ISOC) capable of supporting more than two simultaneous 1-Gbps optical links at 200-km separations with 10^{-9} Bit Error Rate (BER). This work proposes a multiple access scheme that can be implemented in COTS hardware (e.g., FPGA) and meets the performance requirements of the ISOC terminal. Similar protocol developments have been proposed in literature, with the most relevant applied to CubeSat constellations and

978-1-7821-2734-7/20/$31.00 ©2020 IEEE

swarms. Radhakrishnan evaluated Time Division Multiple Access (TDMA) and Code Division Multiple Access (CDMA) performance for satellite cluster communications (downlinks and crosslinks) and found a hybrid TDMA and CDMA system produced maximum throughput, though hardware implementation and applications to optical communication were not discussed [6]. Divsalar analyzed the BER and capacity performance of optical CDMA (OCDMA) in a CubeSat constellation downlinking to a common ground station using Pulse Position Modulation (PPM). The protocol was evaluated in hardware, though a comparison of measured results to simulation was not offered [7]. This work offers a less complex protocol solution for ISOC as well as a pathway to end-to-end hardware implementation.

Following the introduction, section 2 provides a brief overview of the ISOC system, though a full description can be found elsewhere ([8]–[11]). Section 3 of this work presents supporting crosslink budget analysis and relevant system parameters to justify ISOC performance requirements. Section 4 discusses the approach for multiuser operations through a channel access protocol, describes the path forward for hardware implementation, and discusses limiting factors. Lastly, Section 5 concludes this work by summarizing findings.

2. ISOC OVERVIEW

Terminal Architecture

ISOC is a novel lasercom transceiver designed to support multiple simultaneous optical ISLs in CubeSat swarms. The terminal fits in a 1U (10x10x10 cm^3) structure and nominally operates in a 6U bus [8]. The current architecture features an array of transmitters and receivers arranged in a truncated icosahedron geometry giving it quasi-omnidirectional transmit and receive characteristics. Each vertex houses a detector for communications and Angle of Arrival (AoA) estimation for Pointing, Acquisition, and Tracking (PAT). Each face holds a miniature telescope with collimation optics, a MEMS mirror for ±36° beam steering, and high-power laser diode producing 1-W output power at 850-nm.

Mission Overview

Q4 is a technology demonstration mission in which four 6U CubeSats in Low Earth Orbit (LEO) fly in a swarm configuration and use ISOC for OISLs [8]. The cluster's nominal orbit parameters follow an ISS orbit (400-km, 51.6° inclination) with individual spacecrafts slightly offset such that the three outer spacecraft orbit a center, fourth, spacecraft forming a star or hub-and-spoke topology (Figure 1). Intersatellite separations range from tens to a few hundred kilometers and ground station separations from 400-km at nadir to ~1000-km at a 20° elevation. The objective of Q4 is to perform multiple simultaneous crosslinks between spacecraft separated by 200-km at 1-Gbps data rates with BER of 10^{-9}.

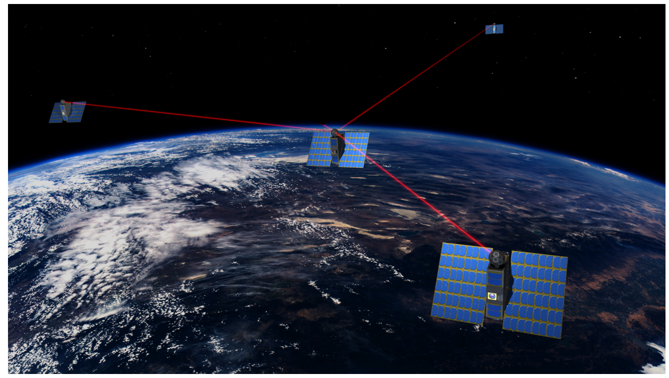

Figure 1: Notional depiction of spacecraft swarm in a star topology equipped with ISOC.

Applications

Q4 is the first step in enabling multiuser laser communications for space-based networks. Future robotic and human exploration missions at Mars or the moon can leverage ISOC capability for communication and navigation. Constellations and swarms in near-Earth environments can incorporate higher levels of autonomy and Delay/Disruption Tolerant Networking (DTN) [12] using ISOC for science observations and data routing.

An example of a science case is the Cubesat Array for Detection of RF Emissions from Exoplanets (CADRE) mission [13]. CADRE uses an array of hundreds to thousands of CubeSats at Earth-Moon L2 to search for exoplanet signatures in the 0.5-30 MHz frequency range using interferometry. Positioned behind the moon, CADRE is shielded from Earth Radio Frequency Interference (RFI) that otherwise distorts measurements in the target spectrum. ISOC is used to transfer observation, position, and timing data between spacecraft for data processing and autonomous operations without corrupting the RFI free zone.

3. LINK BUDGET

A deterministic crosslink budget for ISOC has been developed incorporating flight-like Commercial Off The Shelf (COTS) hardware parameters. Table 1 summarizes the values used for the transmitter, receiver, background noise, and other physical layer assumptions. Individual link performance is sensitive to detector choice, so a worst- and best-case are shown with a PIN and APD, respectively.

Transmitter

Demonstrated CubeSat optical communications use a Master Oscillator Power Amplifier (MOPA) architecture in which a seed laser feeds a doped fiber amplifier [14]. ISOC's volume constraints cannot accommodate the minimum required fiber bending radius for each transmit telescope, thus MOPA is not considered for flight. The considered architecture uses Vertical Cavity Surface Emitting Laser (VCSEL) diode arrays which are commercially available with peak output power levels greater than 2.5-W [15] and sub-nanosecond response times [16]. To keep the power requirements low and link analysis conservative, it is assumed the peak output power is 1-W with uniform intensity over the 3 dB beamwidth.

Table 1: Link Budget Parameter Summary and Resulting Margin

System		
Range	226	km
Wavelength	850	nm
Modulation	PPM-2	-
Data Rate	1	Gbps
BER	1.00E-09	-
Free Space Path Loss	-250.48	dB
Pointing Loss	-3	dB
Background Noise	-120	dBW
Transmitter		
Output Power	0	dBW
Divergence	138.27	μrad
Gain	89.23	dBi
Coating Losses	-1	dB
Receiver		
Effective Aperture Area	17	cm^2
Receiver Gain	104.82	dBi
Coating Losses	-1	dB
Detector	APD	-
Detector Gain	100	-
Responsivity	0.5	A/W
Dark Current	0.1	nA
Excess Noise Factor	3.95	-
Power Received	-71.01	dBW
Power Required	-74.02	dBW
Margin	3.01	-

The transmit telescope aperture size is driven by the throw of the MEMS mirror. At ± 36° optical coverage, 32 distributed transmitters with apertures of 3.6 mm offer full sky coverage will small sections of overlap for handoff. By increasing the throw of the mirror to ± 50° using the Optotune MR-15-30, the number of transmitters can be reduced by half and aperture diameters doubled for better performance.

Receiver

The effective receiver diameter is less than the physical ISOC area because all incident photons along the terminal cannot be collected by detectors alone. Ten to twelve detectors in the truncated icosahedron geometry are visible on any given face not including blind spots introduced by the bus or solar panels. Assuming a minimum incident angle of 30°, the effective area of a bare MarkTech APD 07-005 receiver is 0.22% of the physical area (17.09 mm^2). By adding a biconvex or fisheye lens with a focal length of 10 mm and 6 mm clear diameter, the effective receiver area increases to 31.34% the physical area (25 cm^2).

In the modified transmitter geometry with 7.2 mm diameters, the ~30% physical area assumption holds. While the number of vertices is reduced, more area is available at each point for detector arrays and larger focusing lenses.

Channel

This analysis assumes ISOC uses PPM-2 for both downlink and crosslink. It is well known the free-space optical channel can be modeled with Poisson statistics, however, when the number of photons per bit (PPB) is high, as with the ISOC system, the channel can be modeled as Gaussian [17]–[19]. System noise originates from the detector and front-end electronics (shot, dark, and thermal noise) and background light within the receiver Field Of View (FOV).

Background noise sources include starlight, planet reflections, and solar interference within the system optical bandwidth. All sources will result in increased dark current levels when incident on the ISOC receiver. To mitigate noise current, it is assumed links will occur during eclipse. While this greatly reduces dark current otherwise produced by solar interference, the remaining light increases the noise floor and requires more received power to maintain the same BER and capacity performance.

Figure 2 shows the link range vs margin plot for the given architecture. The intersection of the 3-dB baseline and margin curves determines the maximum range. Using the Optotune MEMS mirror and APD receiver, the maximum range is 204-km and 164-km with a PIN receiver. Parameters for the APD case are itemized in Table 1.

By relaxing the uncoded BER requirement to 10^{-4} and reducing the data rate to 70-Mbps, crosslink separations up to 1003-km can be achieved with the Optotune mirror and APD receiver (Figure 3). Larger separations can be achieved by increasing the transmitter output power or further reducing the data rate.

4. Multiple Access

Access Methods

This analysis evaluates contention-free fixed assignment multiple access protocols to allocate shared medium resources among users. Other multiple access protocols include demand assignment and random assignment; these protocols are not considered due to implementation complexity and performance limitations.

TDMA separates users through orthogonal signaling in time. Each user is assigned a slot in time and may use the full carrier spectrum during transmission (i.e., each user can

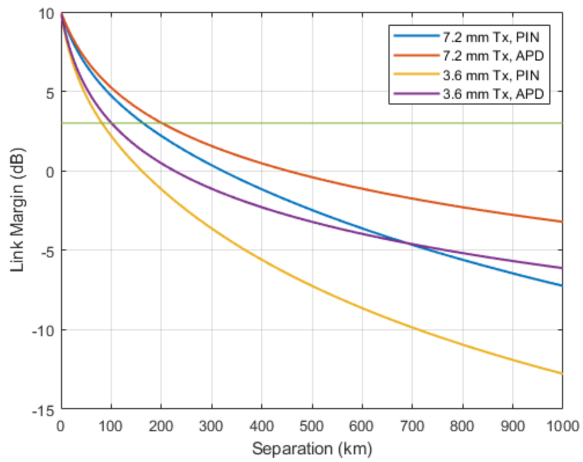

Figure 2: Margin vs Range for ISOC crosslinks at 1-Gbps and uncoded BER 10^{-9}. Desired ranges are achievable with an APD receiver and Optotune MEMS mirror.

transmit at 850-nm at different times). Data arriving at the transmitter after the allocated transmission slot must be queued for the next transmission which introduces an additional latency factor. Strict synchronization between users is required to maintain time orthogonality. The slot time for 1-Gbps PPM-2 rates is 500 ps, meaning minor relative drifts in clock cycles or clock jitter may lead to interfering transmissions. Incorporating a Chip Scale Atomic Clock (CSAC) similar to the CubeSat Handling of Multisystem Precision Time Transfer (CHOMPTT) [20] and Cubesat Laser Infrared CrosslinK (CLICK) [21] missions can enable the precision time required for TDMA. Specific to ISOC, a single user may access the channel at once impeding multiple simultaneous link operation. Introducing user time slots also disrupts continuous communication links, which may lead to insufficient spatial sampling for the PAT system and result in more frequent link acquisitions adding to the delay.

CDMA separates users through orthogonal codes by assigning all users a unique signature sequence optimized for low cross-correlation and high auto-correlation. Using a correlator bank and comparator, the receiver can distinguish signatures in the presence of noise and other user codes, enabling multiple simultaneous link operation. OCDMA was originally developed and implemented in terrestrial fiber systems [22], but the technique has been proposed for CubeSat constellations [7]. This method allows each user to fully utilize time and wavelength spectrum, allows for multiple simultaneous links, and scales with network size. However, using a single user detection receiver, the system is subject to the near-far problem and can only distinguish the user with the strongest receive signal power. To utilize the full benefits of CDMA, a Multi-User Detection (MUD) receiver capable of detecting and demodulating all users simultaneously is required [23]. This introduces considerable signal processing complexity and computational burden on the receiver, thus is not considered further.

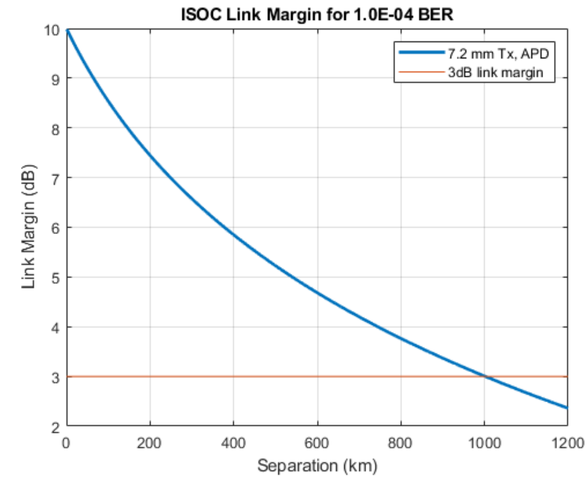

Figure 3: ISOC with relaxed uncoded BER requirement and 70-Mbps data rate can support greater than 1000-km separations between spacecraft

Wavelength Division Multiple Access (WDMA) is analogous to Frequency Division Multiple Access (FDMA) and separates users through orthogonal signaling in wavelength by assigning each user a dedicated frequency from the allocated operating spectrum. With narrow optical bandwidths, users can approach channel capacity and maintain multiple simultaneous links. This method does not scale well with network size as discrete optical trains (i.e., narrowband filter and photodiode) corresponding to user wavelengths are required at the receiver, increasing transceiver SWaP with number of users. An alternative to discrete optical components leveraged by terrestrial fiber networks is photonic technology which actively or passively multiplexes and demultiplexes multiple wavelengths to achieve high channel capacity for lower SWaP [24]. The Technology Readiness Level (TRL) for space-based photonics is low and further analysis and testing are required to determine feasibility for space applications and CubeSat architectures.

Table 2 presents a comparison for the access methods. Each line item represents a desirable characteristic for the access method, and each column is an investigated access method. Green indicates the method has a desired characteristic, yellow shows that under certain conditions, the method has this characteristic but degrades with number of users, and red signals the method does not have this desired trait. Note these aren't mutually exclusive. By combining more than one scheme, the limitations presented by a single method may be solved. For example, a combination Space Division Multiple Access (SDMA) and OCDMA, SDMA and TDMA, or all three results in a system with highly desirable performance and system characteristics.

Despite its shortcomings, this work investigates the feasibility of using TDMA in ISOC. Q4 will have a maximum

Table 2: A comparison of multiple access methods with highlight traits. Note for Wavelength Division, "D" and "P" correspond to discrete and photonics, respectively.

Scheme	Wavelength Division		Code Division	Time Division	Space Division
	D	P			
Capacity per user					
Frequency Utilization					
Time Utilization					
Simplicity					
Scalability					
TRL					
Multiuser Operations					

of four users including the ground station, which is well suited for TDMA. This also enables ISOC to operate within the given power budget and is the least complex to implement. Figure 4 depicts the time-orthogonal signaling format for four users (separated by color) where the assigned time slot is denoted with T_{user}, which is equal to the PPM symbol width T_{sym}, and total TDMA slot width T_{TDMA}.

The PPM channel capacity with noise has been estimated by [25] and is subject to bandwidth, quantum, and noise limitations. Eq. (1) modifies the capacity derived in [25] to account for changes in capacity as a function of number of users, N, which effectively increases the symbol width T_{sym} to the TDMA slot width.

$$C_{TDMA} = \frac{1}{\ln(2)\, E_\lambda}\left(\frac{P_{req}^2}{P_{req}\frac{1}{\ln(M)} + \frac{2\,P_n}{M-1} + \frac{M T_{slot} N P_{req}^2}{\ln(M)\, E_\lambda}}\right) \quad \textbf{(1)}$$

Where E_λ is the photon energy, P_{req} is the power required to close the link from the link budget analysis, M is the PPM order equal to 2 in the case of ISOC, and P_n is the noise power.

The signal to noise ratio (SNR) in a direct-detect lasercom system can be found by squaring the mean photocurrent and dividing by the noise variance. This can also be represented as the effective number of photons, which is the average number of signal photons incident on the detector during an observation interval (e.g., symbol time) reduced by the system noise. The effective number of photons, and therefore SNR, can be represented as photons per bit (PPB) as it incorporates data rate, signal power, and noise power [17].

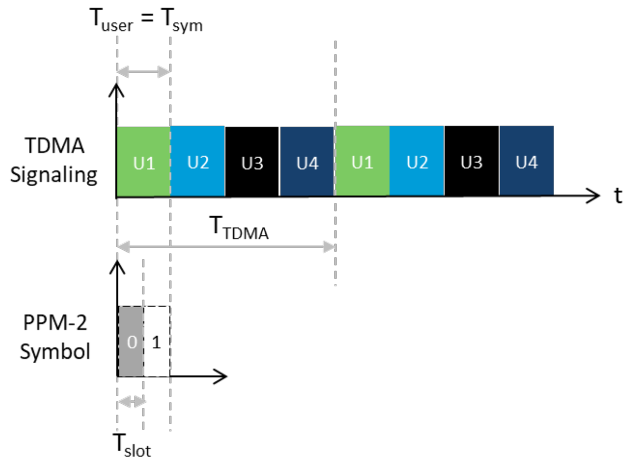

Figure 4: TDMA signal configuration for four simultaneous users (illustrated by color, denoted "UX"). Each user is assigned a unique transmission slot which does not interfere with other users

Figure 5 shows the capacity per user as a function of SNR (PPB) for varying number of users. The result of introducing TDMA into a PPM link is reduced capacity per user because increased slot time introduces T_{sym} $(N-1)$ delay to each PPM symbol translating to a capacity decrease approximately proportional to N inverse. For a slot width of 500-ps (1-ns symbol width for PPM-2), 1-Gbps data rates for a single user can be achieved. Note TDMA capacity is noticeably lower in low SNR scenarios, but saturates at higher SNR across all user cases.

To achieve 1-Gbps data rates using TDMA with 4 simultaneous users, rise and fall times on the order of hundreds of picoseconds are required (Figure 6). While this is within the advertised performance of commercial VCSELs, lab testing is required to verify transmitter performance, and additional feedback loops to monitor and control the modulator will need to be introduced.

Hardware Implementation

An end-to-end transceiver is currently under development for laboratory testing. TDMA will be implemented using an FPGA, such as a Xilinx 7-series device, which can achieve line rates exceeding 10-Gbps using high-speed serial Gigabit Transceiver (GTx) IP cores [26]. The Virtex-7, using the GTX core, supports up to 12.5-Gbps line speeds for up to 36 transceivers with a total bandwidth of 900 GHz. In this context, the FPGA line rate is analogous to baud rate and includes the additional bandwidth required for signal processing. The current architecture multiplexes the received data onto a single digital line to reduce the FPGA computational overhead. In this configuration, a maximum of twelve 1-Gbps simultaneous receive signals can be processed by ISOC.

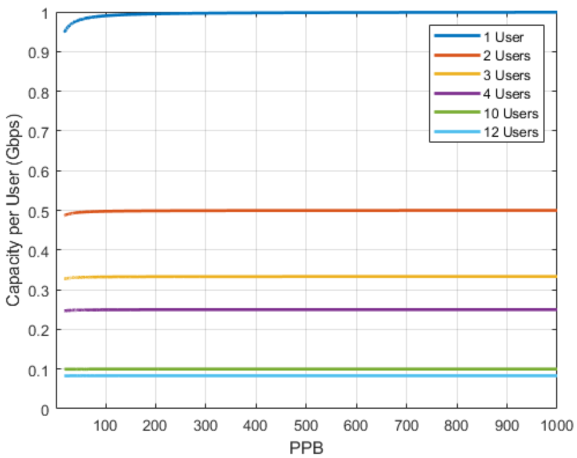

Figure 5: Capacity per user in a TDMA system with 1 ns symbol widths. The maximum achievable data rate scales with ~1/*N* dependence.

Narrow pulse duration and high peak-power using direct-drive modulation presents a unique implementation challenge. High-rate switching in lasers introduces a residual frequency modulation known as chirp which leads to shifts in the operating wavelength, limits extinction ratio (ER), and increases dispersion losses [17]. Compensation via optical filtering and average power-limited amplifiers following the laser output can reduce these effects; however, such an architecture is incompatible with the ISOC terminal. VCSELs may be modulated up to GHz frequencies with fast rise and fall times (~100 ps) and low turn-on delay (~50 ps), but maintaining these specifications requires continuous monitoring of the threshold current (temperature dependent) and tight control of the current bias level (modulation current dependent) [16].

Differential Phase Shift Keying (DPSK) using a Mach-Zehnder Modulator (MZM) is receiving considerable attention and will be used on the upcoming Laser Communication Relay Demonstration (LCRD) [27]. Photodiodes and amplifiers with larger bandwidths will also be required, but this presents less of an architectural challenge as APDs with integrated Trans-Impedance Amplifiers (TIAs) capable of >10-Gbps rates are commercially available [28].

5. Conclusion

ISOC aims to expand laser communication capability by demonstrating multiple simultaneous links for swarms of small spacecraft. The link budget analysis shows that using an APD receiver and transmitter equipped with an Optotune MEMS mirror, data rates of 1-Gbps at uncoded BER of 10^{-9}

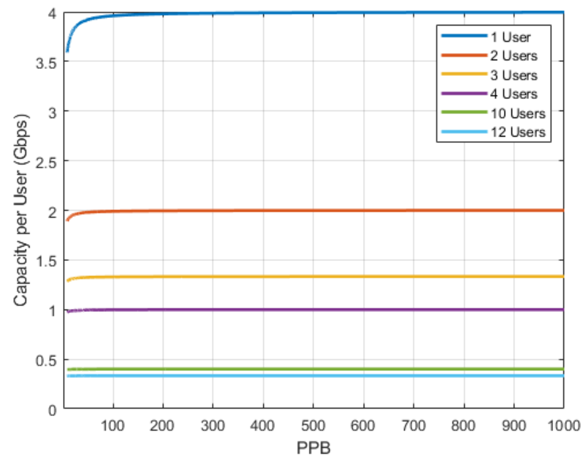

Figure 6: Capacity per user in a TDMA system with 250 ps symbol widths.

are achievable at 200-km ranges. Greater than 1000-km separations are possible by relaxing the uncoded BER requirement and reducing the data rate.

Simultaneous optical links require channel access definition to avoid user interference and data loss. TDMA is analyzed for users operating in an PPM channel with noise. The maximum capacity per user scales inversely with users, and 1-Gbps rates per user are attainable by reducing the symbol rate to 250 ps.

Assuming a TDMA configuration in which one laser operates at a given time, the number of multiple simultaneous links is limited by the FPGA line rate. For the Q4 specific mission architecture, this factor is greater than the number of users and thus does not present as a design driver. In the proposed TDMA and PPM scheme, the limiting factor for capacity is the laser, which operates near the limit of directly-modulated laser.

Acknowledgements

The research was carried out at the Jet Propulsion Laboratory, California Institute of Technology, under a contract with the National Aeronautics and Space Administration. Copyright 2018 California Institute of Technology. U.S. Government sponsorship acknowledged and carried out with funding from NASA's Small Spacecraft Technology Program.

References

[1] Planet, "Products." [Online]. Available: https://www.planet.com/products/.

[2] K. Dowd, "OneWeb's Satellites Deliver Real-Time HD Streaming from Space," 2019. [Online]. Available: https://www.oneweb.world/media-center/onewebs-satellites-deliver-real-time-hd-streaming-from-space. [Accessed: 09-Sep-2019].

[3] C. Henry, “SpaceX launches 60 Starlink satellites, begins constellation buildout.” [Online]. Available: https://spacenews.com/spacex-launches-60-starlink-satellites-begins-constellation-buildout/. [Accessed: 09-Sep-2019].

[4] A. Boyle and T. Soper, “Amazon asks FCC for approval of Project Kuiper broadband satellite operation,” 2019. [Online]. Available: https://www.geekwire.com/2019/amazon-asks-fcc-approval-project-kuiper-broadband-satellite-operation/. [Accessed: 09-Sep-2019].

[5] Telesat, “Telesat LEO - Why LEO?,” 2019. [Online]. Available: https://www.telesat.com/services/leo/why-leo. [Accessed: 09-Sep-2019].

[6] R. Radhakrishnan, W. W. Edmonson, F. Afghah, J. Chenou, and R. M. R.-O. Q.-A. Zeng, “Optimal Multiple Access Protocol For Inter-Satellite Communication in Small Satellite System,” in *The 4S Symposium*, 2014.

[7] D. Divsalar, M. Thill, D. J. Israel, S. Dolinar, M. Shaw, and M. Peng, “Optical CDMA for a constellation of CubeSats,” in *IEEE Aerospace Conference Proceedings*, 2018, pp. 1–11.

[8] J. Sanchez and J. E. Velazco, “Q4 – a CubeSat Mission to Demonstrate Omnidirectional Optical Communications,” in *IEEE Aerospace Conference Proceedings*, 2020.

[9] J. E. Velazco *et al.*, “Inter-satellite omnidirectional optical communicator for remote sensing,” *SPIE Opt. Eng. + Appl.*, vol. 10769, 2018.

[10] U. Zaman, R. Torun, A. Janzen, M. Y. Peng, J. Velazco, and O. Boyraz, “Design Tradeoffs and Challenges of Omnidirectional Optical Antenna for High Speed, Long Range Inter CubeSat Data Communication,” in *SSC18-WKII-06*, 2018, pp. 1–7.

[11] J. E. Velazco, “Omnidirectional Optical Communicator,” in *IEEE Aerospace Conference Proceedings*, 2019, pp. 1–6.

[12] E. Mahoney, “Disruption Tolerant Networking,” 2018. [Online]. Available: nasa.gov/content/dtn.

[13] M. de Kok, J. E. Velazco, and M. J. Bentum, “CubeSat Array for Detection of RF Emissions from Exoplanets using Inter-Satellites Optical Communicators,” in *IEEE Aerospace Conference Proceedings*, 2020.

[14] T. S. Rose *et al.*, “Optical communications downlink from a 1.5U Cubesat: OCSD program,” in *International Conference on Space Optics — ICSO 2018*, 2018, vol. 11180.

[15] FLIR, “High Power VCSEL Arrays: FLIR VCSEL.” [Online]. Available: https://www.flir.com/products/flir-vcsel/.

[16] Finisar Corp, “Application Note Modulating VCSELs,” 2007.

[17] D. O. Caplan, “Laser communication transmitter and receiver design,” in *Journal of Optical and Fiber Communications Reports*, 2007, vol. 4, no. 4–5, pp. 225–362.

[18] H. Hemmati, “Deep Space Optical Communications,” in *Deep Space Optical Communications*, 2006, pp. 1–705.

[19] S. Alexander, “Receiver Performance Analysis,” in *Optical Communication Receiver Design*, 1997, pp. 223–310.

[20] J. W. Conklin *et al.*, “Preliminary results from the CHOMPTT laser time-transfer mission,” in *SSC19-VI-03*, 2019.

[21] K. Cahoy *et al.*, “The CubeSat Laser Infrared CrosslinK Mission (CLICK),” in *International Conference on Space Optics*, 2018, vol. 11180.

[22] J. A. Salehi, “Code Division Multiple-Access Techniques in Optical Fiber Networks - Part I: Fundamental Principles,” *IEEE Trans. Commun.*, vol. 37, no. 8, pp. 824–833, 1989.

[23] S. Verdue, *Multiuser Detection*, 1st ed. Cambridge University Press, 1998.

[24] D. Kilper, K. Bergman, V. W. S. Chan, I. Monga, G. Porter, and K. Rauschenbach, “Optical Networks Come of Age,” *Opt. Photonics News*, pp. 50–57, 2014.

[25] B. Moision and H. Xie, “An Approximate Link Equation for the Direct-Detected optical ppm link,” 2014.

[26] Xilinx, “High Speed Serial,” 2019. [Online]. Available: https://www.xilinx.com/products/technology/high-speed-serial.html#transceivers.

[27] D. O. Caplan *et al.*, “Ultra-wide-range Multi-rate DPSK Laser Communications,” in *Optics InfoBase Conference Papers*, 2010, pp. 1–2.

[28] Lumentum, “Avalanche Photodiode (APD) 10G Chip.” [Online]. Available: https://www.lumentum.com/en/products/avalanche-photodiode-10g-chip-PA006700.

BIOGRAPHY

Alexa Aguilar *received a B.S. in Electrical Engineering from the University of Idaho in 2017 and Master of Science in Aerospace Engineering from the Massachusetts Institute of Technology in 2019. She is currently leading the optical communication protocol development effort for the Inter-Satellite Omnidirectional Optical Communicator (ISOC) terminal at JPL and pursuing her Ph.D. in Aerospace Engineering at MIT. Prior to JPL, she worked for Facebook, Inc. and MIT Lincoln Laboratory.*

Dr. Jose Velazco *is JPL's principal investigator for the Omnidirectional Optical Communicator and has over 20 years of experience in carrying out R&D projects. Dr. Velazco has extensive experience in implementing wideband receivers for electronic surveillance applications including wide-open and superheterodyne receivers where he acquired expertise in direction-of arrival (Direction Finding) hardware and software. Recently he worked on an advanced multimegabit Optical communicator for ground application and on an all-digital phase-array radar. He is currently working jointly with University of Michigan on the design of a small CubeSat constellation mission for testing various network protocols. In addition, he is developing a gigabit Omnidirectional Optical Communicator at JPL. Dr. Velazco's current interest include the implementation of spacecraft swarms and formation flying as well as all optical spaceborne networks. He is also the technical supervisor of JPL's Advanced RF and Optical Technology Group, which develops advanced communications microwave and millimeter-wave transmitters, as well as high sensitivity receivers for NASA's Deep Space Network.*

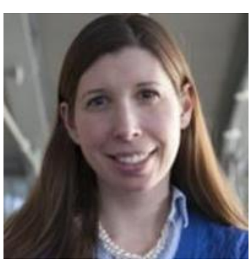

Prof. Kerri Cahoy *is an Associate Professor of Aeronautics and Astronautics at MIT and leads the Space Telecommunications, Astronomy, and Radiation (STAR) Laboratory. Cahoy received a B.S. (2000) in Electrical Engineering from Cornell University, and M.S. (2002) and Ph.D. (2008) in Electrical Engineering from Stanford University. Dr. Cahoy previously worked as a Senior RF Communications Engineer at Space Systems Loral, and as a postdoctoral fellow at NASA Ames. Cahoy currently works on nanosatellite atmospheric and ionospheric sensing missions (MicroMAS, NASA TROPICS, AERO/VISTA), optical communications (NASA CLICK), and exoplanet technology demonstration (DARPA DeMi) missions.*